

ON WAVELET BASED ENHANCING POSSIBILITIES OF FUZZY CLASSIFICATION METHODS

Submitted: 20th October 2018; accepted: 2nd June 2020

Ferenc Lilik, Levente Solecki, Brigita Sziová, László T. Kóczy, Szilvia Nagy

DOI: 10.14313/JAMRIS/2-2020/18

Abstract:

If the antecedents of a fuzzy classification method are derived from pictures or measured data, it might have too many dimensions to handle. A classification scheme based on such data has to apply a careful selection or processing of the measured results: either a sampling, re-sampling is necessary. or the usage of functions, transformations that reduce the long, high dimensional observed data vector or matrix into a single point or to a low number of points. Wavelet analysis can be useful in such cases in two ways.

As the number of resulting points of the wavelet analysis is approximately half at each filters, a consecutive application of wavelet transform can compress the measurement data, thus reducing the dimensionality of the signal, i.e., the antecedent. An SHDSL telecommunication line evaluation is used to demonstrate this type of applicability, wavelets help in this case to overcome the problem of a one dimensional signal sampling.

In the case of using statistical functions, like mean, variance, gradient, edge density, Shannon or Rényi entropies for the extraction of the information from a picture or a measured data set, and they don not produce enough information for performing the classification well enough, one or two consecutive steps of wavelet analysis and applying the same functions for the thus resulting data can extend the number of antecedents, and can distill such parameters that were invisible for these functions in the original data set. We give two examples, two fuzzy classification schemes to show the improvement caused by wavelet analysis: a measured surface of a combustion engine cylinder and a colonoscopy picture. In the case of the first example the wear degree is to be determine, in the case of the second one, the roundish polyp content of the picture. In the first case the applied statistical functions are Rényi entropy differences, the structural entropies, in the second case mean, standard deviation, Canny filtered edge density, gradients and the entropies.

In all the examples stabilized KH rule interpolation was used to treat sparse rulebases.

Keywords: Fuzzy classification, wavelet analysis, fuzzy rule interpolation, structural entropy

1. Introduction

Real-life control or classification problems are often solved by fuzzy methods, as fuzzy inference is usually practically more efficient, flexible and close to the human way of thinking than classical, crisp decision schemes. As the digital measuring and picture taking

devices become more and more widespread, the measured data becomes larger, contains more information about the measured or photographed objects, but most of the such acquired information disturbs an automatic control or classification scheme. For training a neural network or other, nature based learning method, however, very large number of measurement with time and resource consuming pre-processing is often needed, thus in some cases it is not possible to use them.

Digital measuring devices sample either in time, like in the case of an oscilloscope or temperature monitoring system; in frequency, like in the case of spectrum analysers; or in space, like in the case pictures or 3D scanners. The results of such measurements often consist of several hundreds or thousands or even millions of points, but such large data sets are not suitable for serving as the antecedent set for a fuzzy decision or classification scheme.

The measured data has to be made processable by a fuzzy inference system of reasonable size and complexity, mostly by decreasing the amount of data with the condition of keeping as much information as possible. The simplest step to achieve this may be re-sampling: selecting only a few from the measured values as representatives of the whole data set. A more sophisticated method would be averaging. However, both lead to loss of information. From image and data compression it is well known that wavelets are suitable for distilling a lot of the available information and achieving a large compression ratio, thus it seems to be reasonable to try wavelet transform for achieving suitable compression rate as well as sufficiently small information loss. In case of telecommunication line insertion loss over frequency functions, this method proved to be effective.

Instead of wavelet-based compression of the measurement results, its useful information content can be extracted by calculating statistical parameters, like its mean value, standard deviation, average gradient or gradient direction, some kind of shape-related quantity or its entropy, or entropies, if Rényi's generalisation of the definition of entropy is used. In the case of pictures edge densities or colour related parameters might be also necessary. Rényi's generalised entropies can be combined into such quantities that characterise the shape or topology of the measured distribution, too, this step can map the measured data into a couple of points. This scheme is useful especially in the case of two- or three-dimensional measured data, as the number of measured points is usually too high, and

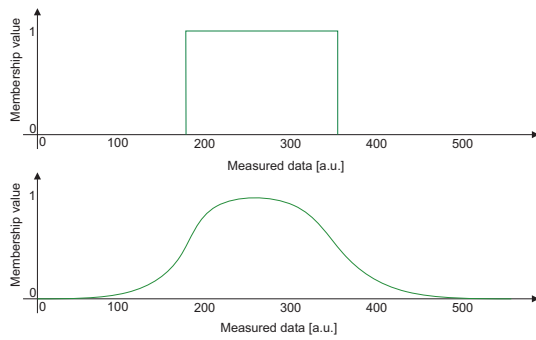


Fig. 1. Crisp and fuzzy membership function of a measured variable

the number of the remaining points is still too high after wavelet-based compression. In many cases, using only entropies, or other, similar functions leads to critically high information loss, thus a method for regaining some of the information should be introduced. As the high-pass filter outputs of the wavelet transform distill the fine details from the original data and the low-pass outputs behave as a kind of averaging, applying the same functions – the previously mentioned statistical parameters and entropies – on the wavelet transformed versions of the images leads to other information. This step can enhance the performance of an inference system without increasing the number of antecedents too much. This scheme proved to be efficient in significantly increasing the effectiveness of a classification scheme in surface roughness and color-rectal polyp content characterisation.

These two approaches are studied in the following considerations. As a first step, in Sec. 2a summary about fuzzy classifications is given completed with a section of fuzzy rule interpolation. Next the introduction of wavelet transforms is given in Sec. 3. Sec. 4 gives the generalization of the Shannon entropy and its use in the characterisation of shapes of functions or distributions. The applicability of the first approach is demonstrated in Sec. 5, and the usage of wavelet transform for increasing the information content is given in Sec. 6 and Sec. 7. A conclusions to be found in the last section.

2. The Fuzzy Component of the Approach

2.1. Fuzzy Sets

In set theory L.A. Zadeh came forth with a new concept in 1965. According to his idea [1], an element can not only be fully member of a set, or fully not member of it, but there can be infinite many possibilities inbetween. This concept is closely related to the human way of thinking, as there is a smooth transition between a tea being hot or cold, or a dog breed being small, medium-sized or large. Zadeh's fuzzy sets do not only allow membership values of exclusively 0 or 1 (like with the traditional, crisp sets), but any value in the $[0, 1]$ unit interval. A measured value can have a membership degree in a fuzzy set, thus it also becomes a fuzzy quantity, as it can be seen in Fig. 1 Based on such fuzzy sets, decisions can be made, like "IF

the water level is low", "THEN fill the water tank with a small amount of water", or "IF the temperature is high", "THEN classify it to the highest class". In the case of multiple conditions, like "IF the gasoline concentration is high AND the pressure is high" it is necessary to re-define the operators "AND" and "OR". Zadeh defined "AND" as the lowest of the membership values (called nowadays rather *t-norm*), and "OR" as the highest (called *s-norm* or *t-conorm*).

2.2. Fuzzy Inference

Using the fuzzy membership functions a rather flexible control systems can be built. Mamdani proposed [2] the first concept for carrying out fuzzy control (and decisions), which was a computationally more efficient implementation of the Compositional Rule of Inference method also proposed by Zadeh [3]. His concept used multiple input variables, i.e., antecedents. For each of the outputs, i.e., consequents, he defined a set of rules, consisting of membership functions for all the antecedents. The consequent fuzzy set arises as the *s-norm* (e.g., maximum) of the results for consequents, and the results for a consequent is the *t-norm* (e.g., minimum) of the rules belonging to that consequent, as it can be seen in Fig. 2.

The rules are generated from measured data, either using statistics or some intelligent learning algorithm. This means that there must be some measurements, where not only the antecedents, but also the consequents are known, moreover, it is useful to have such data for testing the inference system. In our examples very simple rules are used: the membership function of each antecedent for each consequent is a triangle, with the minimum and maximum of the measured data forming the support of the membership function and the mean forming the core, the peak of the triangle, as seen in Fig. 3.

2.3. Fuzzy Rule Interpolation

In measurements it often happens that the rule-base does not completely cover the space of the possible measured data, i.e., sparse rulebases are generated. In this case, making the other measured data evaluable can be carried out by rule interpolation. Stabilized KH interpolation [4], [5], [6]

$$\inf\{B_{\alpha}^*\} = \frac{\sum_{i=1}^{2n} \left(\frac{1}{d_{\alpha L}(A^*, A_i)} \right)^k \inf\{B_{i\alpha}\}}{\sum_{i=1}^{2n} \left(\frac{1}{d_{\alpha L}(A^*, A_i)} \right)^k} \quad (1)$$

$$\sup\{B_{\alpha}^*\} = \frac{\sum_{i=1}^{2n} \left(\frac{1}{d_{\alpha U}(A^*, A_i)} \right)^k \sup\{B_{i\alpha}\}}{\sum_{i=1}^{2n} \left(\frac{1}{d_{\alpha U}(A^*, A_i)} \right)^k} \quad (2)$$

give very good results in our examples, too.

3. The Wavelet Component of our Approach

Wavelet analysis [7] developed from several branches of signal processing and numerical mathematics in the late 1970s-early 1980s. Up till now its main use is image compression, from fingerprint databases

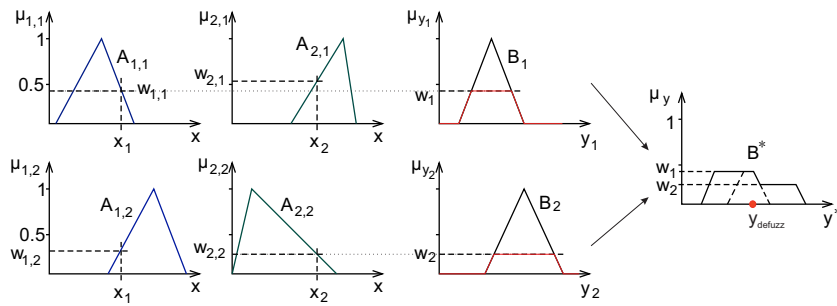


Fig. 2. Mamdani's fuzzy consequent from a two-dimensional antecedent and two consequent sets. The rules are denoted by the membership values $A_{i,j}$ of the variable x_i , the consequent sets by B_{y_j} , and the final consequent set by B^* . The final consequent is usually defuzzified, thus one value y_{defuzz} becomes the result of the inference. Arbitrary units

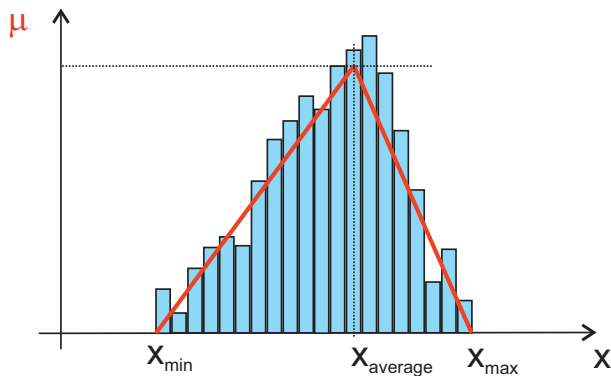


Fig. 3. A simple rule generation method from the measured values of the training set. The statistics of the measured data is represented by the histogram of the plot, while the resulting fuzzy rule by the triangle-shaped membership function. Arbitrary units

through the Mars rover [8] to the JPEG2000 image coding standard [9]. It is also possible to suppress noise, enhance edges, or retrieve special types of patterns from images by wavelet transform, moreover, similarly to Fourier transform [10], wavelets are used to simplifying differential equations, too [11].

3.1. Multiresolution Analysis

The discrete wavelet transform is mathematically defined by a so called multiresolution analysis of the function space, mostly the square integrable functions' Hilbert space. It consists of subspaces embedded into each other, each subspace belonging to a resolution level, hence the name. The finest resolution level subspace is dense in the original function space (i.e., to any function of the original function space to any limit there can be found a function in the infinitely fine resolution subspace that is closer than the limit). The lowest (infinitely low) resolution level consists of only constant functions.

The most interesting part of this approach of the function space is that each subspace is expanded by a set of basis functions, which have the same shape, just shifted over a regular grid. The shape of the basis functions change from subspace to subspace, i.e., from resolution level to resolution level only by shrinking or dilation: the fine resolution level subspaces have higher and narrower basis function distributed over

a grid of smaller grid distance, while the rougher resolution levels have lower, wider basis functions over grids with larger grid distance, as it can be seen from the following definitions of the basis functions at resolution level j and shift position k

$$\phi_{jk}(x) = 2^{j/2} \phi(2^j x - k). \quad (3)$$

These basis functions ϕ_{jk} of the embedded subspaces are called scaling functions.

Wavelets are also similar basis functions: they provide the way between two resolution levels. The spaces completing a rougher resolution level subspace to the next, finer resolution subspace are the detail spaces, and their basis functions are the wavelets, defined as

$$\psi_{jk}(x) = 2^{j/2} \psi(2^j x - k). \quad (4)$$

This subspace setup means, that any function of any resolution level j can be expressed either as a linear combination of its resolution level subspace, or using any rougher resolution level scaling function subspace as a basis, and adding wavelets to it as a refinement, i.e., as

$$f^{[j]}(x) = \sum_{-\infty}^{\infty} c_{jk} \phi_{jk}(x), \quad (5)$$

or by decreasing the basic resolution level by 1 as

$$f^{[j]}(x) = \sum_{-\infty}^{\infty} c_{j-1,k} \phi_{j-1,k}(x) + \sum_{-\infty}^{\infty} d_{j-1,k} \psi_{j-1,k}(x), \quad (6)$$

or by decreasing the rougher resolution level to zero, as

$$f^{[j]}(x) = \sum_{-\infty}^{\infty} c_{0k} \phi_{0k}(x) + \sum_{i=0}^{j-1} \sum_{-\infty}^{\infty} d_{ik} \phi_{ik}(x), \quad (7)$$

Practically, measurement results can be treated as a very fine resolution level coefficient set of the sampled function, their wavelet transform results in the rougher resolution level scaling function and wavelet coefficients by using the so called refinement equation

$$\phi(x) = 2^{1/2} \sum_{i=0}^{N_s} h_i \phi(2x - i), \quad (8)$$

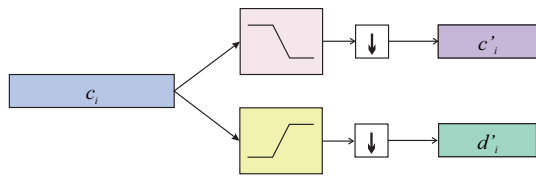


Fig. 4. One step of the wavelet transform as two branches of convolutional filter signal processing and downsampling steps. The low-pass filter results in the scaling function expansion coefficients c'_i , while the high-pass filters give the fine details, i.e., the wavelet expansion coefficients d'_i

and its wavelet counterpart

$$\psi(x) = 2^{1/2} \sum_{i=-N_s+1}^1 (-1)^i h_{-i+1} \phi(2x-i). \quad (9)$$

For the simplest wavelet family, the so called Haar wavelets [12], the coefficients $h_0 = h_1$, these mother basis functions have a support length 1 unit; the other wavelets have more coefficients, thus longer support.

3.2. Wavelet Analysis in Signal Processing

This mathematical definition can be translated to signal processing devices: practically the usage of (8) and (9) can be translated directly to digital signal processors as convolutional filtering and downsampling, as it can be seen in Fig. 4. The coefficients in the convolutional filters are proportional to the coefficients at the refinement equations.

In multiple dimension data sets either multiple dimension wavelets, or more often separate wavelet analysis steps in the separate dimensions has to be carried out.

4. Entropies as Compact Descriptions of Two-Dimensional Datasets

The entropy in information theory was introduced by Shannon [13] as the expectation value of the information for a complete set of events, i.e., for such sets, where all the events have probabilities between 0 and 1, and the sum of all the probabilities is 1. If the probabilities are $\{p_1, p_2, \dots, p_N\}$, then the entropy can be written as

$$S = - \sum_{i=1}^N p_i \log_2 p_i. \quad (10)$$

4.1. Rényi Entropies

Shannon's entropy definition was generalised for many purposes, Rényi's [14] series of entropies, i.e.,

$$S_\alpha = \frac{1}{1-\alpha} \log \sum_{i=1}^N p_i^\alpha, \quad (11)$$

gives the Shannon entropy as a limit at $\alpha = 1$.

For $\alpha = 0$ this entropy is the entropy of the uniform distribution. This is sometimes called Hartley entropy, as Hartley has introduced the concept of information and its expectation value using such set, where

the probabilities were equal. This approximation is still used if nothing is known about the probability distributions, only the number of the possible outcomes.

For $\alpha = 2$ the formula turns into

$$S_2 = - \log \sum_{i=1}^N p_i^2. \quad (12)$$

4.2. Structural Entropies of Probability Distributions

In the beginning of the 1990s Pipek and Varga [15], [16] found out, that the difference of Rényi entropies can characterize the structure of the probability distribution $\{p_1, p_2, \dots, p_N\}$ in a very peculiar way. They introduced structural entropy as the difference of two Rényi entropies

$$S_{str} = S_1 - S_2, \quad (13)$$

and similarly, they proved that the so called filling factor q , which was used in solid state physics and quantum mechanics, is also related to a Rényi entropy difference the following way

$$\log(q) = S_0 - S_2. \quad (14)$$

Later these quantities were applied in characterisation of the localisation of pixel intensities in scanning microscopy images [17], [18]. Bonyár developed a localization factor for describing the roughness of gold electrodes based on these entropy differences [19], [20]

5. Telecommunication Lines

5.1. Measurements

In telecommunication line performance prediction the goal is to develop a method that approximates the real-life performance of the line sufficiently well, without actually building the connection, as it is costly and time consuming. For SHDSL lines, which are mainly for business use, errors in the prediction lead to financial loss to the telecommunications provider. Lilik measured over 170 lines [21], and developed a fuzzy method for performance prediction [22], [23].

During the measurements the SHDSL links were built, and their performances were measured. Also many physical parameters were determined using general measuring devices available at telecommunications service providers. Sorting out the noise, the return loss and many other parameters, it was proved that based on solely the insertion loss values of an area's telecommunications lines their performance can be evaluated with rather high reliability. The measured insertion loss values over the 0 to 2 MHz frequency band can be seen in Fig. 5.

5.2. Characterisation Scheme

In order to be able to build a classification method, the measured data was separated to a training set and a test set. In the original characterisation scheme simple, triangular rules were built from the measured data of the training set according to Fig. 3. As the insertion loss values have rather large fluctuations around

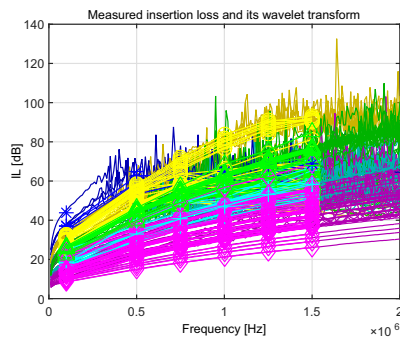


Fig. 5. Measured insertion loss as a function of frequency for the lines of the 5 performance groups. The darker shades of colours mean the measured lines properties, while the brighter counterparts denote the wavelet transforms

a quite smooth trend, five characteristic frequencies were chosen, and the insertion loss values at those frequencies served as antecedents. Selecting fewer frequency points makes the calculations unstable, more points make it unnecessarily complicated. Still, there were a lot of lines that were not evaluable, and there were very few cases, when the fluctuations were so bad, that the evaluation was not successful, i.e., instead of sorting the line into its real performance group, or one group below it (which is still acceptable for the provider), it sorted it to better performing group or predicted much worse data rate than the real one.

For overcoming these problems, as a first step, we introduced fuzzy rule interpolation to our classification scheme, thus making practically all the lines evaluable.

Instead of selecting five representative samples from the complete insertion loss-frequency function, we also applied wavelet analysis to filter out the large-scale trends from the function. The first wavelet transform we use can also be seen in Fig. 5. It can be seen, that the distribution of the transformed points is not equidistant: in the lower frequency domain we included one step finer resolution level results than in the higher frequencies, because the communication's spectral power density is much larger at lower frequencies.

65 lines were used for testing, in the case of the characteristic frequencies, 12 lines were put to one class lower than their real group, while in the case of the wavelet transformed antecedent selection 8 lines went to the acceptable group and the remaining 57 ones to their true classes. In both cases all the lines were classified well, moreover, if the wavelet transform was carried out until 2 or 4 points remained, the classification was still as correct as the 5-point version [23].

With these results we demonstrated that wavelets can be used for stabilising calculations, if the measured data fluctuates and lowering the antecedent dimension as well.

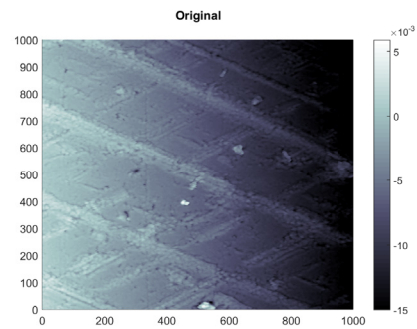


Fig. 6. A measured surface segment before wavelet analysis

6. Wear

If the number of the antecedent dimensions is already too low, like in the case of classification based on the S_{str} and $\ln q$ values calculated for an image, wavelets can provide 4 more pictures to be analysed, as it can be seen in Fig. 6 and Fig. 7. In 2D data sets the wavelet analysis is carried out in both dimensions. This results in 4 output pictures of approximately quarter of the size of the original data set (half in each direction), one output for the case of using low-pass filters in both dimensions, which is a kind of average of the original image, two outputs where one of the directions have low-pass, the other high-pass filter, and one output where both filters are high-pass. In the followings the latest picture will be called diagonal, the first averaging, and the two between will be mentioned as vertical and horizontal results, depending on which direction has the fine details, i.e., which direction used high-pass filter.

6.1. Measurements

In [24] Solecki and Dreyer measured a combustion engine using silicone replica and surface scanners. Silicone replicas are often used in geometrical measurements as the shape of many instruments does not allow to access certain interesting points of an object. In the case of a combustion engine the inner surface of the cylinders can be accessed only by specially designed devices that are not available in general laboratories, but they are developed exquisitely for one type of automated measurement in the industry. These highly specialized tools are expensive thus if hardly accessible surfaces are to be measured, either the object has to be cut, or replicas are to be taken from the surface. If the object under test is needed for further tests, clearly only the second option is possible.

The measurements of the 4 cylinders of the engine under test were carried out using Struers RepliSet F5 which is able to reproduce patterns of size down to 0.1 microns. Replicas were taken of the new engine before building it and after 500 hours of polycyclic endurance test (later the engine was cut so that the worn surface could be studied directly, as well). The resulting samples were measured by a TalysurfCLI2000 white-light surface scanner at 5 points for each of the cylinders. These points were selected so that one point would

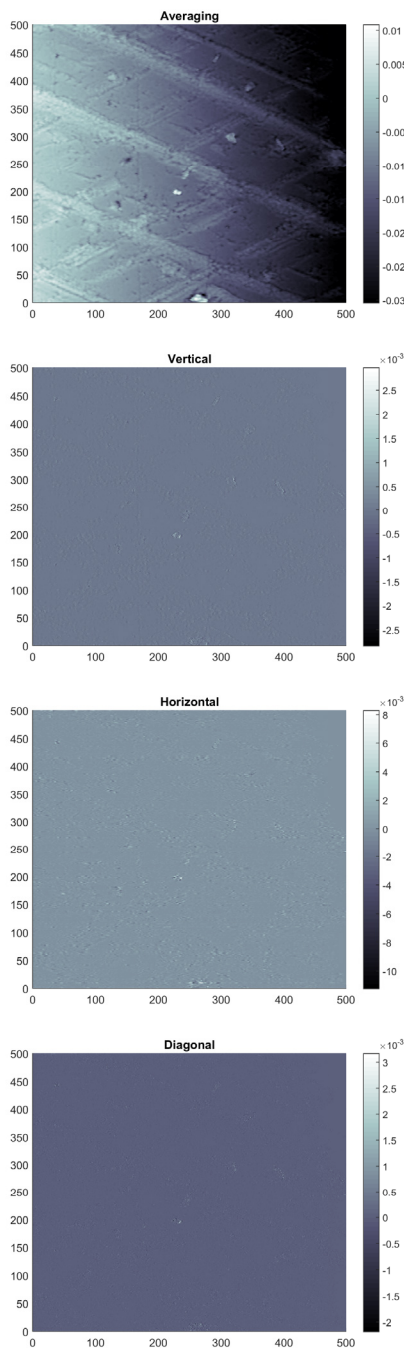


Fig. 7. A measured surface segment after wavelet analysis

be between the topmost and the second ring's turning point, another point would be between the next two piston rings's turning points, and three along the path where all 3 piston rings had worn the surface. An example of the 1 mm by 1 mm surface parts of a new and worn engine can be seen in Fig. 8. Slight vertical scratches can be seen on the worn surface. Such a vertical scratch can be seen in the previous worn image of Fig. 6, too, and slightly visible in the vertical transformed picture of Fig. 7.

6.2. Characterisation Scheme

The classification scheme was very similar to the one in the previous section. The antecedents consist

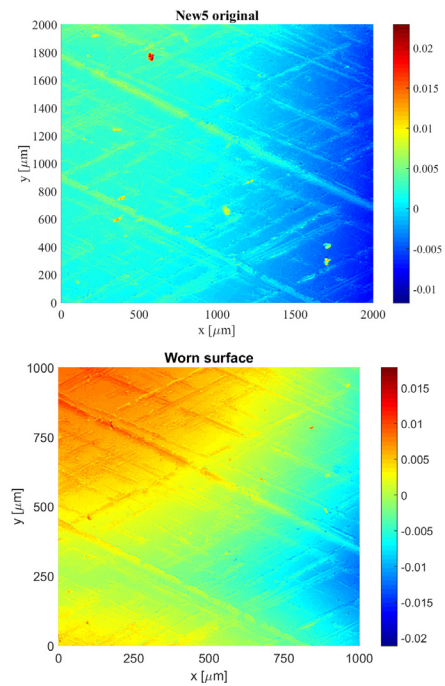


Fig. 8. A measured surface segment before and after the polycyclic endurance run

ted of solely the structural entropy and the logarithm of the filling factor, i.e., the two Rényi entropy differences. The $S_{str}(\ln q)$ plot of 128 measured surface sub-domains are plotted in Fig. 9. It can be seen, that though the points corresponding to worn and new surfaces occupy overlapping domains, there are clearly such parts of the plot which belong to only one type of surface.

However, these two characterising quantities are not sufficient for building fuzzy classification scheme: from the 128 surface subdomains 64 were used for building the rulebase, and of the 64 test data, only 33 could be classified correctly, which is worse than a random guess.

In the case of two-dimensional data, such as the above surface scans, wavelet transformation has to be carried out in both dimensions, thus resulting in 4 output data matrices: one for the transformation, where both directions had low-pass filters, one for the high-pass-high-pass case, and two mixed filter pairs. The structural entropy and the filling factor can be calculated for all 4 of the resulting matrices, thus the antecedent dimension can be increased from 2 to up to 10. We tested [25] the method with all 4 wavelet transformed surface types as well as with only the low-pass-low-pass and high-pass-high-pass matrices, and the results were not different from each other. The number of incorrectly classified surface elements went down to 13, which indicates, that the structural entropies are not suitable for being antecedents without other quantities. The second wavelet transform usually does not improve the results in this example.

However we could demonstrate that wavelet analysis is able to introduce independent information to the overly simplified antecedents.

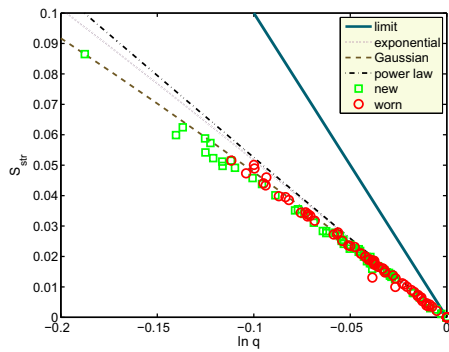


Fig. 9. Structural entropy map of 64 new and 64 worn surface segments. This is a typical way of plotting structural entropy, and determining the localization type of the studied distribution. The teal thick solid line denotes the theoretical limiting curve, above which no points should appear. The dashed, dotted and dash-dotted lines shows three typical distributions, i.e., if a point is near the line corresponding to the 2nd order power law distribution (dash-dotted), then the average localization type in the distribution is similar to the second order power law function. The green squares give the points generated from the new surfaces's scans, while the red circles the worn ones

7. Colorectal Polyps

Colorectal polyps are wart-like objects inside the last parts of the bowel system. Some of these polyps can develop into colorectal cancer, which is a really dangerous type of cancer, as it can be detected usually quite lately. If these polyps, that have the possibility to develop into cancer could be detected and removed early, then they would not develop into malign objects, thus detecting and classifying colorectal polyps is a really important task. Having a visual aid for the medical experts based on automatic image processing can help the diagnosis. There are several groups trying to find polyps on colonoscopy images, some of them even have their own database built. In the following considerations, we apply our method founded in [26] on the pictures of [27]. An example can be seen in Fig. 10, while the wavelet transform of the picture is given in Fig. 11.



Fig. 10. A colonoscopy picture of [27] turned into grayscale image, before wavelet analysis

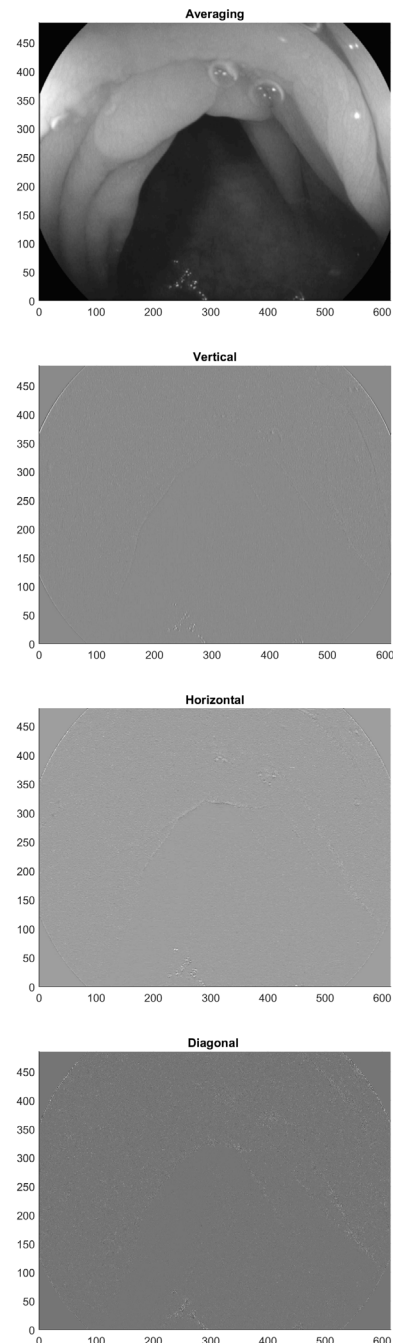


Fig. 11. Colonoscopy picture after wavelet analysis. Note that the upper left corner of the picture in Fig. 10, i.e., the pixel of index (1,1) moved to the lower left part of the coordinate system (the picture is upside down)

The classification scheme consists of the following steps. First, the images are cut into tiles of size $N \times N$, where N is generally between tenth and fifth of the original image size, in our case 200 compared to the image size of magnitude 1000. Next, using the masks provided by the database, for each tile the polyp content, i.e., the percentage of the area with masked pixels is calculated: based on this value the tiles are classified as "with polyp" and "without polyp". For each of the tiles, for all 3 colour channels the antecedents were calculated. The antecedents are the mean, standard deviation, edge density, structural entropy and $\ln q$ and

the gradients. The edge density is calculated the following way: the tile is transformed to a black and white edge image by Canny filtering, then the rate of the edges (white points) compared to the tile-size.

Next, every second image is used for determining the fuzzy rules according to Fig. 3. As our previous experiences show, that for different types of images the classification success rates are different, we sorted the pictures into groups of the same patient of the same take, and generated rules from each of the groups. The thus arising rules are applied for classification using the same method as in the case of the cylinder surfaces, only the antecedent dimension increased to 21, or 99 in the case of using wavelet analysed pictures, too.

The results for both cases can be seen as ROC plots in Fig. 12. The Classical ROC plots are not that much visible due to the large number of points, however, if a 3rd axis, i.e., the image group number is also given, we can conclude the followings. The false positive rate is rather low in all cases, especially in the case of using wavelet analysed images, too. The true positive rate is for some pictures extremely low, so this method without wavelet analysis is not usable, however, wavelets improve the results up to a more acceptable level in all cases.

8. Conclusion

In this articles the usage of wavelet transform in fuzzy antecedent selection was studied. Two completely different strategies were mentioned. First, the simplification of the decision and decrease of the number of antecedents by using wavelet transform instead of samples form a measured data vector, which scheme's effectiveness was demonstrated on insertion loss-based performance prediction of telecommunication lines. Second, the introduction of new, independent information by using wavelet transformed data beside the original one for classification schemes with overly simplifying antecedent selection such as selecting structural entropies. Combustion engine cylinder surface scan classification was used as a demonstrating example, where the performance of the classification could be improved significantly by introducing two of the wavelet transforms of the surface matrix. The other example was colonoscopy picture segment classification, where the improvement due to wavelet analysis was more visible, and to almost all the image types the classification error rate became acceptable.

ACKNOWLEDGEMENTS

The authors would like to thank the financial support of the projects GINOP-2.3.4-15-2016-00003 and the ÚNKP-18-4 New National Excellence Programme of the Ministry of Human Capacities of Hungary. This work was supported by National Research, Development and Innovation Office (NKFIH) K124055. The authors would like to thank to EFOP-3.6.1-16-2016-00017 1 "Internationalisation, initiatives to establish a new source of researchers and graduates, and development of knowledge and technological transfer as

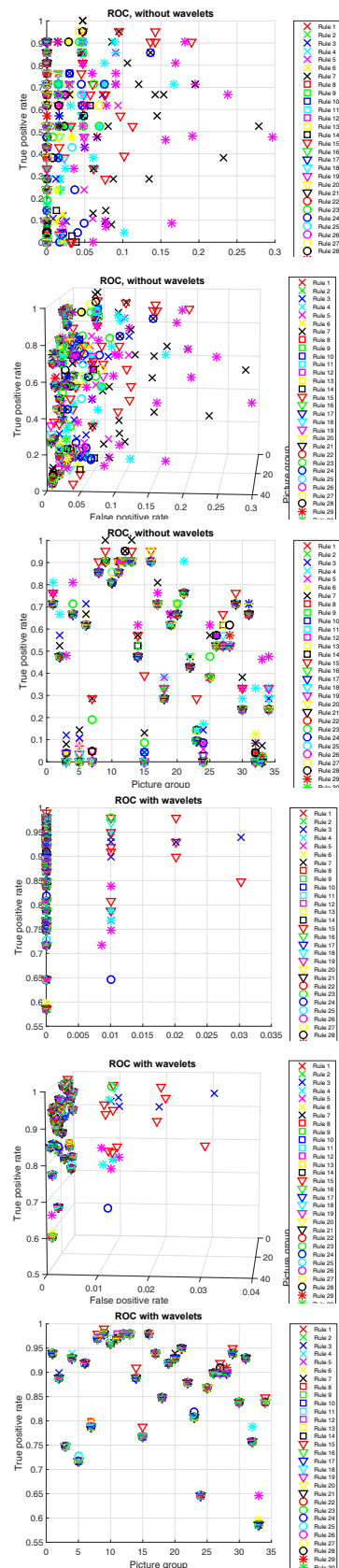


Fig. 12. True positive vs false positive rate for the various picture groups for the various rulebases. First plot is the ROC, the second is a 3D view, and 3rd plot focuses on true positive rate. First row: without wavelet analysis, 21 antecedents, second row: with wavelet analysis, 99 antecedents

instruments of intelligent specialisations at Széchenyi István University” for the support of the research.

AUTHORS

Ferenc Lilik* – Széchenyi István University, H-9026 Győr, Egyetem tér 1, e-mail: lilikf@sze.hu.

Levente Solecki – Széchenyi István University, H-9026 Győr, Egyetem tér 1.

Brigita Sziová – Széchenyi István University, H-9026 Győr, Egyetem tér 1.

László T. Kóczy – Széchenyi István University, H-9026 Győr, Egyetem tér 1.

Szilvia Nagy – Széchenyi István University, H-9026 Győr, Egyetem tér 1.

*Corresponding author

REFERENCES

- [1] L. Zadeh, “Fuzzy sets”, *Information and Control*, vol. 8, no. 3, 1965, 338–353, 10.1016/S0019-9958(65)90241-X.
- [2] E. Mamdani and S. Assilian, “An experiment in linguistic synthesis with a fuzzy logic controller”, *International Journal of Man-Machine Studies*, vol. 7, no. 1, 1975, 1–13, 10.1016/S0020-7373(75)80002-2.
- [3] L. A. Zadeh, “Outline of a New Approach to the Analysis of Complex Systems and Decision Processes”, *IEEE Transactions on Systems, Man, and Cybernetics*, vol. SMC-3, no. 1, 1973, 28–44, 10.1109/TSMC.1973.5408575.
- [4] L. Kóczy and K. Hirota, “Approximate reasoning by linear rule interpolation and general approximation”, *International Journal of Approximate Reasoning*, vol. 9, no. 3, 1993, 197–225, 10.1016/0888-613X(93)90010-B.
- [5] L. Kóczy and K. Hirota, “Interpolative reasoning with insufficient evidence in sparse fuzzy rule bases”, *Information Sciences*, vol. 71, no. 1-2, 1993, 169–201, 10.1016/0020-0255(93)90070-3.
- [6] D. Tikk, I. Joó, L. Kóczy, P. Várlaki, B. Moser, and T. D. Gedeon, “Stability of interpolative fuzzy KH controllers”, *Fuzzy Sets and Systems*, vol. 125, no. 1, 2002, 105–119, 10.1016/S0165-0114(00)00104-4.
- [7] I. Daubechies, *Ten Lectures on Wavelets*, CBMS-NSF Regional Conference Series in Applied Mathematics, Society for Industrial and Applied Mathematics, 1992, 10.1137/1.9781611970104.
- [8] A. Kiely and M. Klimesh. “The ICER progressive wavelet image compressor”. https://ipnpr.jpl.nasa.gov/progress_report/42-155/155J.pdf, 2003, Accessed on: 2020-09-18.
- [9] C. Christopoulos, A. Skodras, and T. Ebrahimi, “The JPEG2000 still image coding system: an overview”, *IEEE Transactions on Consumer Electronics*, vol. 46, no. 4, 1103–1127.
- [10] J.-B.-J. Fourier, *Théorie Analytique de la Chaleur*, Firmin Didot: Paris, 1822.
- [11] S. Nagy and J. Pipek, “An economic prediction of the finer resolution level wavelet coefficients in electronic structure calculations”, *Physical Chemistry Chemical Physics*, vol. 17, no. 47, 2015, 31558–31565, 10.1039/C5CP01214G.
- [12] A. Haar, “Zur Theorie der orthogonalen Funktionensysteme (On the theory of orthogonal function systems, in German)”, *Mathematische Annalen*, vol. 69, no. 3, 1910, 331–371, 10.1007/BF01456326.
- [13] C. E. Shannon, “A mathematical theory of communication”, *The Bell System Technical Journal*, vol. 27, no. 3, 1948, 379–423, 10.1002/j.1538-7305.1948.tb01338.x.
- [14] A. Rényi, “On Measures of Entropy and Information”. In: *Proceedings of the fourth Berkeley Symposium on Mathematics, Statistics and Probability*, 1961, 547–561.
- [15] J. Pipek and I. Varga, “Universal classification scheme for the spatial-localization properties of one-particle states in finite d-dimensional systems”, *Physical Review A*, vol. 46, no. 6, 1992, 3148–3163, 10.1103/PhysRevA.46.3148.
- [16] I. Varga and J. Pipek, “Rényi entropies characterizing the shape and the extension of the phase space representation of quantum wave functions in disordered systems”, *Physical Review E*, vol. 68, no. 2, 2003, 026202, 10.1103/PhysRevE.68.026202.
- [17] I. Mojzes, C. Dominkovics, G. Harsányi, S. Nagy, J. Pipek, and L. Dobos, “Heat treatment parameters effecting the fractal dimensions of AuGe metallization on GaAs”, *Applied Physics Letters*, vol. 91, no. 7, 2007, 073107, 10.1063/1.2768911.
- [18] L. M. Molnár, S. Nagy, and I. Mojzes, “Structural entropy in detecting background patterns of AFM images”, *Vacuum*, vol. 84, no. 1, 2009, 179–183, 10.1016/j.vacuum.2009.04.025.
- [19] A. Bonyár, L. M. Molnár, and G. Harsányi, “Localization factor: A new parameter for the quantitative characterization of surface structure with atomic force microscopy (AFM)”, *Micron*, vol. 43, no. 2, 2012, 305–310, 10.1016/j.micron.2011.09.005.
- [20] A. Bonyár, “AFM characterization of the shape of surface structures with localization factor”, *Micron*, vol. 87, 2016, 1–9, 10.1016/j.micron.2016.05.002.
- [21] F. Lilik and J. Botzheim, “Fuzzy based Prequalification Methods for EoSHDSL Technology”, *Acta Technica Jaurinensis*, vol. 4, no. 1, 2011, 135–144.
- [22] F. Lilik, S. Nagy, and L. T. Kóczy, “Wavelet based fuzzy rule bases in pre-qualification of access

- networks' wire pairs". In: *AFRICON 2015*, Addis Ababa, Ethiopia, 2015, 1–5, 10.1109/AFRICON.2015.7332034.
- [23] F. Lilik, S. Nagy, and L. T. Kóczy, "Improved Method for Predicting the Performance of the Physical Links in Telecommunications Access Networks", *Complexity*, 2018, 3685927, 10.1155/2018/3685927.
- [24] M. R. Dreyer and L. Solecki, "Verschleissuntersuchungen an Zylinderlaufbahnen von Verbrennungsmotoren". In: *3. Symposium Produktionstechnik – Innovativ und Interdisziplinär*, Zwickau, 2011, 69–74.
- [25] S. Nagy and L. Solecki, "Wavelet Analysis and Structural Entropy Based Intelligent Classification Method for Combustion Engine Cylinder Surfaces". In: *Proceedings of the 8th European Symposium on Computational Intelligence and Mathematics, ESCIM*, Sofia, 2016, 115–120.
- [26] S. Nagy, F. Lilik, and L. T. Kóczy, "Entropy based fuzzy classification and detection aid for colorectal polyps". In: *2017 IEEE AFRICON*, 2017, 78–82, 10.1109/AFRICON.2017.8095459.
- [27] J. Silva, A. Histace, O. Romain, X. Dray, and B. Granado, "Toward embedded detection of polyps in WCE images for early diagnosis of colorectal cancer", *International Journal of Computer Assisted Radiology and Surgery*, vol. 9, no. 2, 2014, 283–293, 10.1007/s11548-013-0926-3.